

Design and Execution of a DC Source with High Power and High Efficiency

Alhassan Musa Oruma¹

University of Greenwich

Department of Electrical and Computer Engineering
Master's Degree

Stephen Olatoye Olaniyan²

University of Greenwich

Department of Electrical and Computer Engineering
Master's Degree

Vincent Ojomaje Anyah³

New Mexico Highlands University

Department of Computer Science
Master's Degree

Abstract:- Powering the modern world requires increasingly efficient energy conversion systems. This paper presents the design and step-by-step implementation of a high-efficiency DC-DC power converter for DC drive motor applications. A flyback converter circuit uses MOSFETs, capacitors, transformers, and microcontrollers to provide well-regulated DC output voltage through calculations, simulations, and testing. Key stages explained include the AC-DC conversion and rectification, flyback transformer with PWM control, and output regulation. Extensive MATLAB and Proteus software simulations evaluate anticipated performance before constructing the hardware converter. Testing with oscilloscopes compares real-world results against design goals for voltage regulation and efficiency. The paper demonstrates that careful engineering design and testing enable building a functional, high-efficiency DC-DC converter with 95-100% measured efficiencies. Overall, this work details the process of creating an efficient power electronics system for motor drive applications, from calculations to software simulations to hardware implementation.

Keywords:- DC Source, High Power, High Efficiency, Converter, Rectifier, Transformer, Metal Oxide Field Effect Transistor (MOSFET), Microcontroller, Flyback, Pulse Width Modulation (PWM), Simulation and Printed Circuit Board (PCB).

I. INTRODUCTION

This paper presents the design and implementation of a high-efficiency DC power converter for DC drive motor applications. The thesis is that through careful component selection and calculations, simulations, and testing, an efficient DC-DC converter can be constructed to provide well-regulated DC output voltage. Keywords related to this paper include DC-DC converter, flyback converter, power electronics, pulse width modulation (PWM), microcontroller, rectifier, transformer, and efficiency. Specifically, this paper details the step-by-step process for constructing the converter, including the calculations and

equations used to select proper components like MOSFETs, capacitors, inductors, resistors, and diodes to build the rectifier, filter, flyback transformer, and regulation stages. Extensive simulations were conducted in MATLAB and Proteus software to model the anticipated performance before construction. Finally, the paper presents results from real-world testing using oscilloscopes to characterize the efficiency and voltage regulation achieved compared to the design goals. The thesis is that careful design and testing yield a functional, high-efficiency DC-DC converter for motor drive applications.

➤ *Step of Design and Component Selection*

The circuit component calculations in this section are done to prevent needless harmful situations.

• *Complete Rectifier for Bridges*

A complete bridge rectifier contains four diodes within a closed loop with an AC voltage as the base; with this type, the case would lead to an AC voltage that pulses DC voltage. This project uses two sets of two half-thus; the bridge rectifier helps rectify the single-phase Alternate Current input voltage that will then be filtered (to be made ride in ripple to rectified DC). This could be done by determining the total output of the home full bridge rectifier of Amara Enterprises. = $1.414 \times 230 = 325V$.

• *Convertor Flyback*

The single-phase flyback converter represented the DC converter and its buck-boost. Arrangement. The resistor flyback is the best-known topology for low-power arrangements in the power supply design. To make it more attractive to customers, three main features in flyback topology are simple design and cost-effectiveness, allowing output to have high efficiency to be taken into consideration. The usage of Alternate to Direct and Direct Current to Direct Current converters includes self-operating, high-voltage transfer lines like power installations at homes, buck converters in switching modes, power spectrum in the power lab, and the power conversion of optical equipment.

The factors that determine how the flyback converter will perform and operate, even with relatively high efficiency, are usually high levels of input and output, ripple currents, etc. The PWM or microcontroller is also used for the operation of the components. The single-phase AC fed through the rectifier is converted to DC, where the voltage is controlled at the flyback output level. The LCR filter follows after connecting the high-frequency transformer to eliminate ripple and improve the smooth output voltage. The pulses of the PWM pulse are held in the presence of a MOSFET switch control system by turning the gate on and off for the levelling output voltages. The flyback comprises power mosfet switches as in the IR2101 N-Channel 3 Pins type.

• *Transformer*

Flyback transformers are becoming increasingly popular because of their efficiency, low cost, and straightforward design. The flyback transformer provides isolation between the primary and secondary windings, allows for multiple outputs, and enables selecting either a positive or negative output voltage, unlike similar circuits without these capabilities. Transformers intended for high-frequency power applications must meet specifications like minimizing loss mechanisms and offering a suitable cooling plan. The primary goal is to reduce the core losses, to which close attention must be paid and requires making appropriate choices regarding the switching frequency, core material, and form and size. The primary distinction is found in selecting the core size and form. A solid grasp of proximity losses and skin effects is necessary to minimize copper losses at high frequencies.

• *Filter Design*

AC voltage at the converter and load, which appears across (flyback) output terminals, will have certain ripples that need to be eliminated through a special filtering arrangement. In such a case, a passive primary filter acting like a reactance pole with an inductor upstream and a subsequent capacitor is enough. This setup will cause a current to almost the entire opposition of 2 mm.

The choice of inductance and capacitor is presented by formulation where d-a circuit reactance with ($\omega L + \frac{1}{\omega C}$) functioning as the resonant circuit at $\omega = \frac{1}{\sqrt{LC}}$

For C is one mF, the value L becomes 13.2mH....Equation 1

• *PIC 16F690*

The microcontroller PIC16F690 with two pins for generating the complementary sign was derived using such case PWM. Another key feature is its compatibility with producing PWM output for comparing capture registers. In control applications, PIC microcontrollers are the most preferred items as these possess some features like improved power efficiency, faster speed of operation, and low cost. The above complementary push-pull, which is centrally aligned, is also referred to as the proper independent mode supported by the microcontroller. This microcontroller incorporates advanced analogy features like a high-speed analogue-to-digital converter with versatile trigger modes that connect to required signals for ADC conversions. It provides PWM to drive DC/DC, AC/DC, PFC inverters and lighting systems. PIC microcontroller is usually used to improve the frequency stability of power converters operating at high frequencies within the system. Employer pin mistakes are taken as the subsequent forms are mentioned below:

Table 1 Pin Arrangement for PIC16F690

Pin Number	Full Name	Function
1	Voltage Drain Drain (VDD)	Ground pin
2	Clock Input (CLK IN)	The inputs of the oscillator crystal
3	Clock Output (CLK OUT)	
4	Master Clear (MCLR)	Configuring the voltage input
5	Capture Compare Pulse Width Modulation 1 / Pulse Width Modulation A (CCP1/PWM1A)	Pulse Width Modulation signals
6	Pulse Width Modulation B (PWM1B)	Pulse Width Modulation signals
7	Pulse Width Modulation C (PWM1C)	Pulse Width Modulation signals
14	Pulse Width Modulation D (PWM1D)	Pulse Width Modulation signals
17-19	Register A0-Register A2 (RA0-RA2)	Input voltage

II. MOSFET DRIVER (MD)

The IR2101 gate driver accepts the low-power input from the microcontroller and converts it into a high-current gate drive signal required to turn on the MOSFET properly. Since MOSFETs are high-precision devices with low switching losses, the gate signal must provide enough current to exceed the gate threshold voltage for the ON state. The PWM signals from the microcontroller have an insufficient current to drive the MOSFET gate directly for the correct operation of the controlled plant. Therefore, the gate driver acts as an interface providing the necessary high

current gate signal based on the low-power PWM input. This transitory, weak signal results in the worse performance of the device due to power loss and slow switching caused by this signal. To simplify this, the device goes wrong, the hardware overheats and draws too much current, and these are the only primary failings.

In addition, packages that include a gate driver compensate for one need to drive the switches so that their operation is correct. The gate driver IR2101 receives a low-power input from the microcontroller and converts it into the high-current gate drive signal required to operate the

MOSFET. Due to this ability to transform a low-power control signal into the high-current capability needed for the MOSFET, the complementary mode of the IR2101 was

chosen as the interface for the flyback power MOSFETs. The layout is shown here at the bottom.

Table 2 Descriptions of Pins for MOSFET Driver

Pin Number	Purpose
1	Energy source (5V)
2	high PIC16F690 input level
3	Low PIC16F690 input.
4	Ground
5	low H bridge output
6	Not related
7	Elevated Output to H Bridge
8	Not related

The second implementation was based on the MATLAB/Simulink simulation control for the flyback converter.

DC voltage output monitoring of the DC motor needs to be performed to avoid sudden changes in the production process, causing the DC motor to have shorter primitive times. The PIC microcontroller develops a voltage pulse to activate the switch. The PIC weighs have a pulse of 050% duty ratio. The voltage in the primary transformer varies with the change in the process duty ratio, which ranges from zero to fifty per cent. Before the comparator is implemented, PI control will be used to compute the pulses suitable for the MOSFET fly-black converter and, hence, to form the PWM signals. This will be the microcontroller's details. The microcontroller MATLAB implemented together with V ref operated at producing an error of the observed DC voltage. The analogue to the digital converter of the selected microcontroller has eight bits for converting DC voltage.

➤ *Application of Programming for Microcontrollers*

The PIC16F690 microcontroller has been programmed for the fly-black implementation in this project. The microcontroller's ability to output PWM via the TIMER2 control pin is one of its valuable capabilities. The PWM period is calculated: PR2 assigned with 407.16 and prescaler set with 4.

$$\text{Period}(PR2) = [\text{Clock frequency}/(4 \times \text{mode} \times \text{PWM frequency})] - 1$$

$$\begin{aligned} \text{Period} (PR2) &= [8 \times 10^6 / (4 \times 1 \times 4.9 \times 10^3)] - 1 \\ &= 407.16 \end{aligned}$$

The variation in the duty cycle requires that the variation is proportional regarding CCPRIL. Hence, the CCPRIL conversion of v, for voltage:

$$i = \frac{PR2}{256} \times 256 \times \text{Duty cycle}$$

The microcontroller must have an algorithm and code written to be programmed. The appendix section has a detailed code listing.

➤ *Implementation of Converters*

The flyback converter is implemented once the hardware design stages are finished. The flow chart explains the steps and method of implementation.

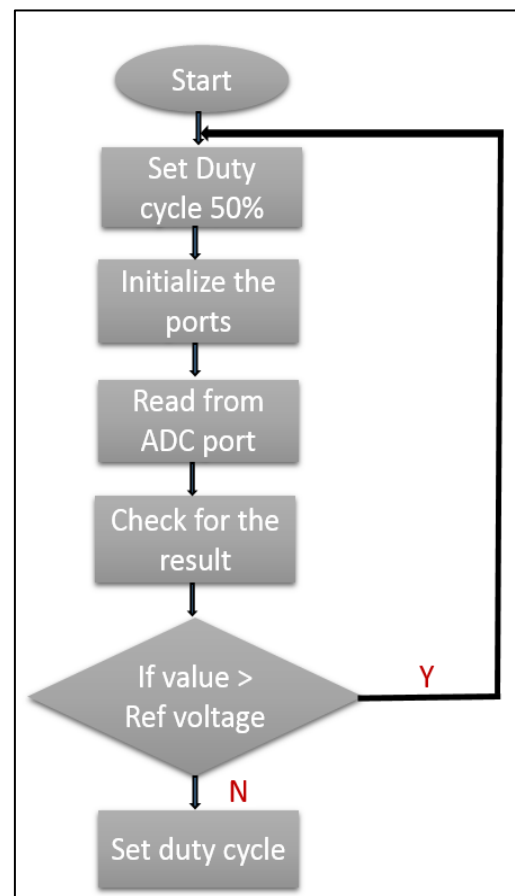


Fig 1 Flow Chart

The microcontroller is designed to function in the steps outlined in the above flow chart, depending on the desired DC output voltage. The microcontroller was programmed to modify the duty cycle and frequency to meet the desired values.

The PICkit 3 debugger and Gate Software programmer tools were utilized to program the microcontroller. The MPLAB programming software, which offers a setting for creating microcontroller programs, was in charge of this

debugger. The six-pin debugger is subsequently connected to the converter PCB through a six-pin connector, and the chosen debugger supplies the controller's power. Consequently, the controller was switched on the debugger. This process started with the dsPIC programming that produced a PWM pulse from the microcontroller.

However, by selecting a specific channel, the microprocessor generated the output PWM signal that ran the MOSFET gate. The main job of this signal is to cause

the MOSFET to be involved in the transformer. The pin low in PWM1 was chosen to determine the PWM channel. Channel 1 produced the standard PWM signals involving the production of the low and high ones at various pins. Initially, these signals were designed to research the channels using them to interpret behaviour, leading to the ultimate understanding of behaviour and its associated relationships. The characteristics of the PWM signal have been programmed to initiate it in a certain percentage at the start and increase it with time.

III. MATLAB IMPLEMENTATION

MATLAB software has been employed to do some simulations, and the computed and assumed frequency values for the circuits shown in the following figures were entered into the program;

The MATLAB implementation diagram for the AC input full bridge rectifier is displayed in Figure 2. Four diodes are connected in the diagram to create two positive sinusoidal voltage halves. To get the best voltage, a capacitor is attached to the output.

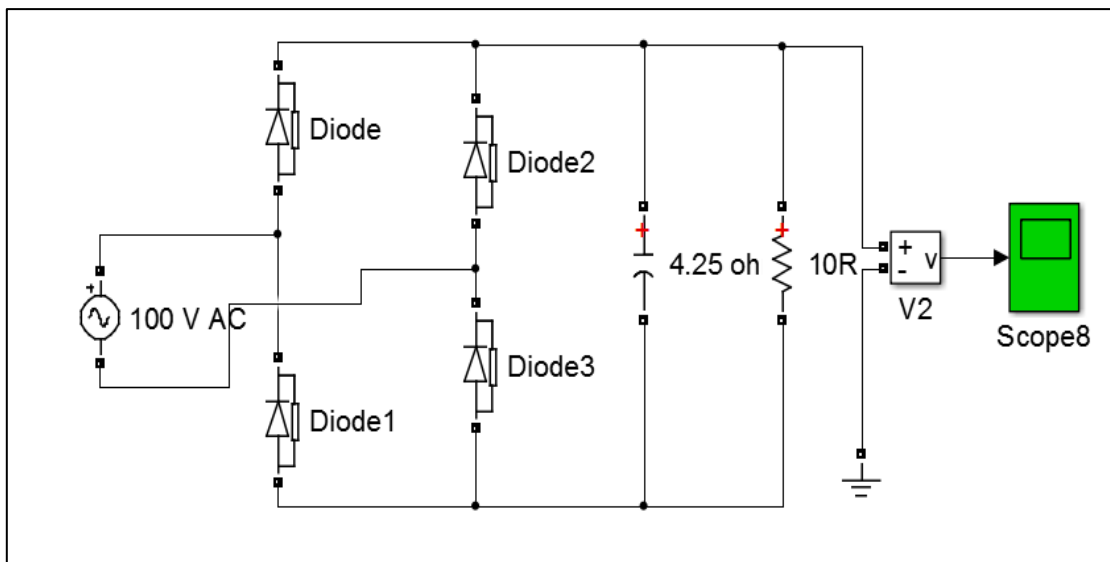


Fig 2 Shows the Diagram of the Bridge Rectifier as Given in whole MATLAB Circuit

Figure 3 is a MATLAB block diagram showing the Flyback converter's implementation. Both transformers are mutual so that 150V output will satisfy the DC load motor.

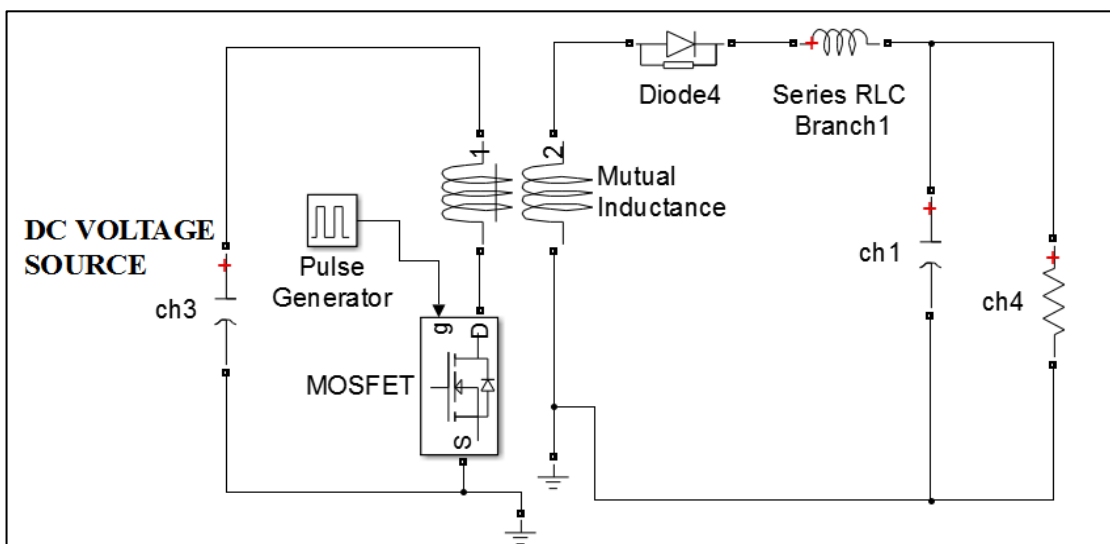


Fig 3 MATLAB Circuit Diagram of the Flyback Converter Circuit

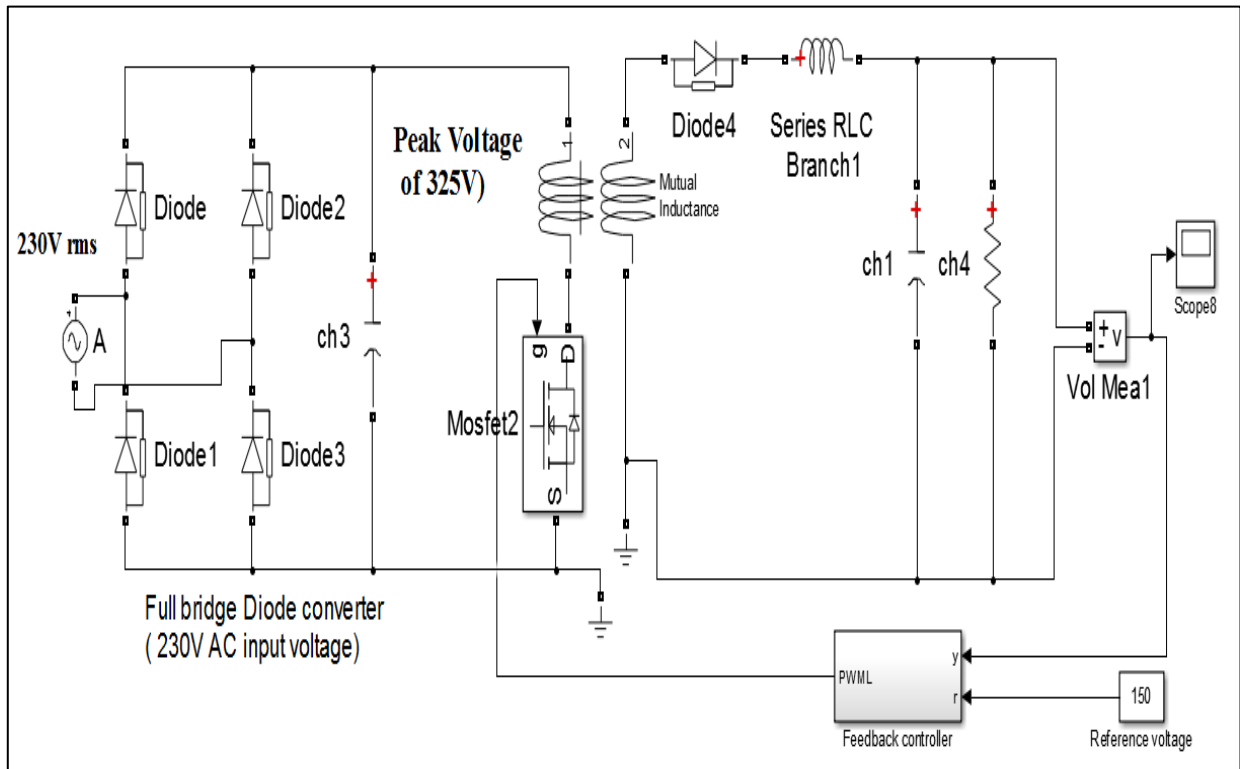


Fig 4 Converter with High-Frequency Transformer

A high-efficiency square-wave signal produced by the flyback converter was transferred via the high-frequency transformer. The square-wave signal is converted back to DC voltage by the bridge rectifiers and stored in the L1+C2 intermediate circuit, where it is smoothed out before being supplied into the load or public grid.

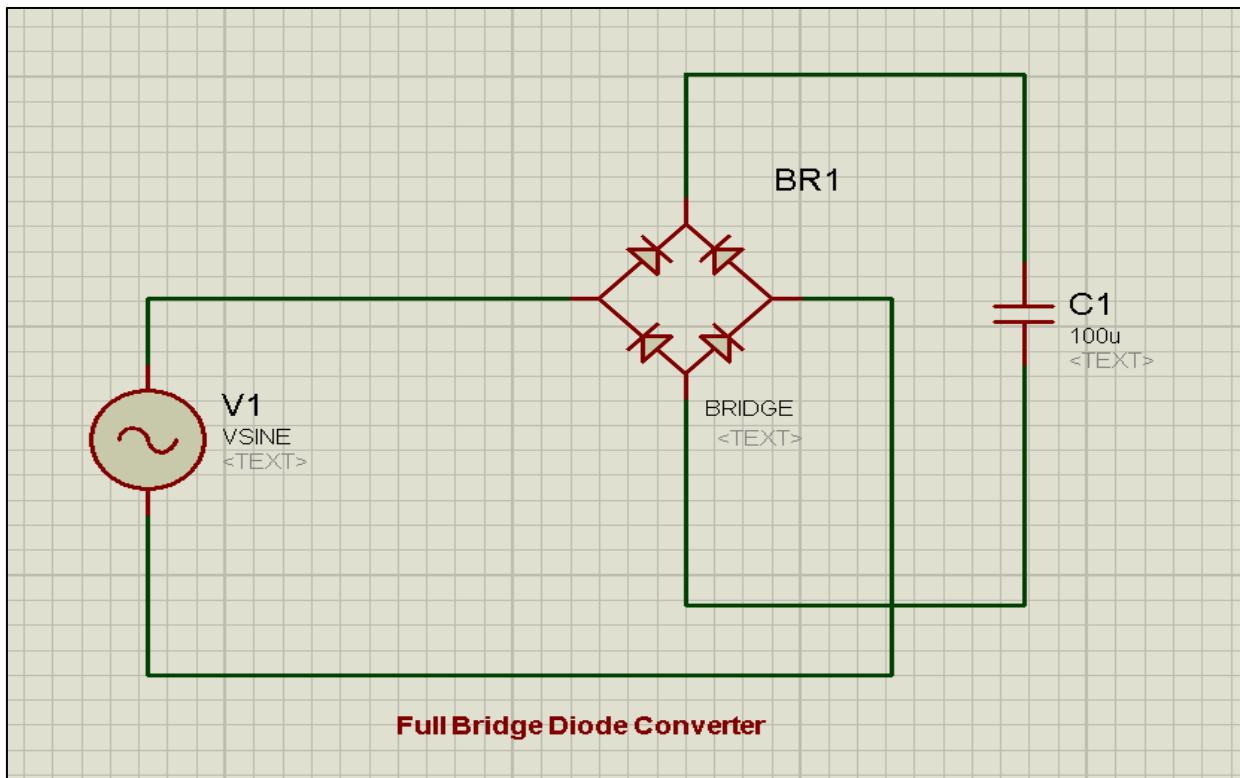


Fig 5 The Complete Bridge Rectifier Converter Secondary Circuit Diagram

Figure 6 represents the ISIS simulation (ISIS 2009) of the transformer circuit for the flyback converter; the flyback converter provides rectifier MOSFET, transformer, diode, and filter elements. The transformer is non-ideal; therefore, the voltage output (150V) will serve the needed load element, a DC motor.

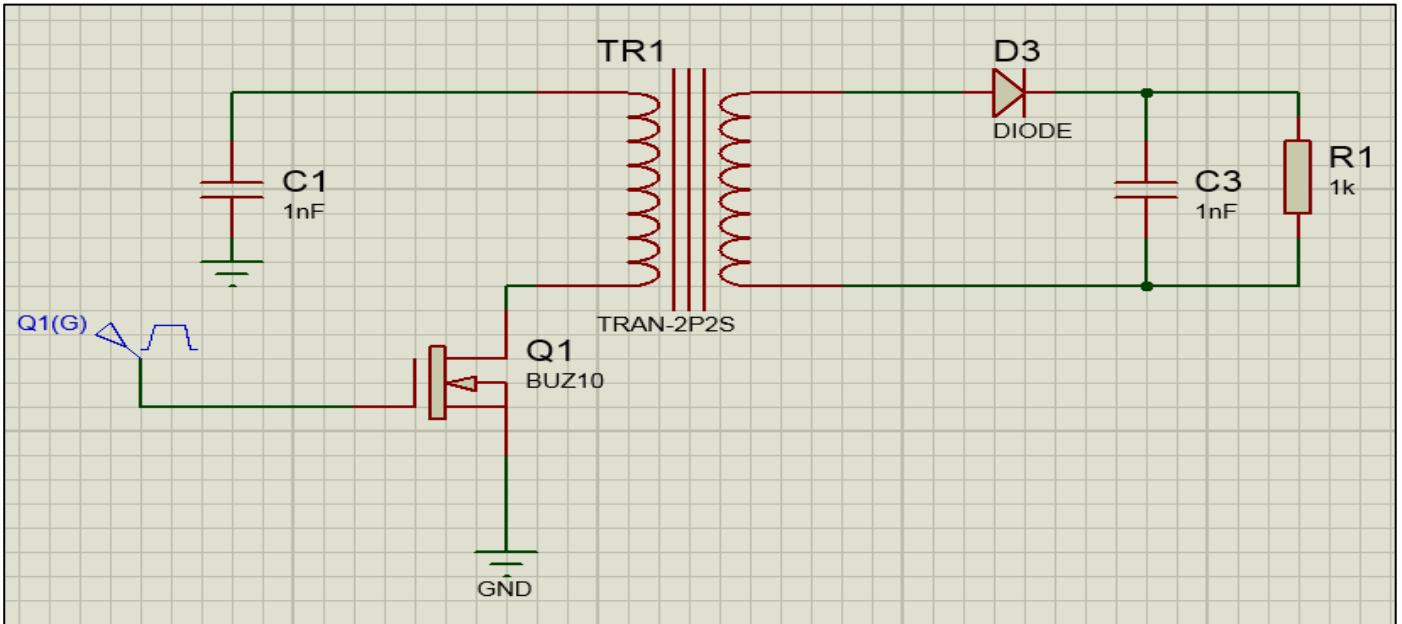


Fig 6 Proteus Computer Simulation Software Circuit Diagram of the Flyback Converter

All the multiple energies are projected to the secondary winding, and good efficiency flyback can be better simulated based on ISIS and illustrated in Figure 5.8. The energy stored in the magnetizing inductance was transferred to the secondary winding when the switch was turned on due to the uninterrupted power flow to the capacitance. This enabled energy transfer at a low cost. The magnetizing energy was transferred to the secondary and multiplied by two when the switch was off. The advantage of using a converter with high efficiency is well-known in the circuit since it minimizes losses in the circuit.

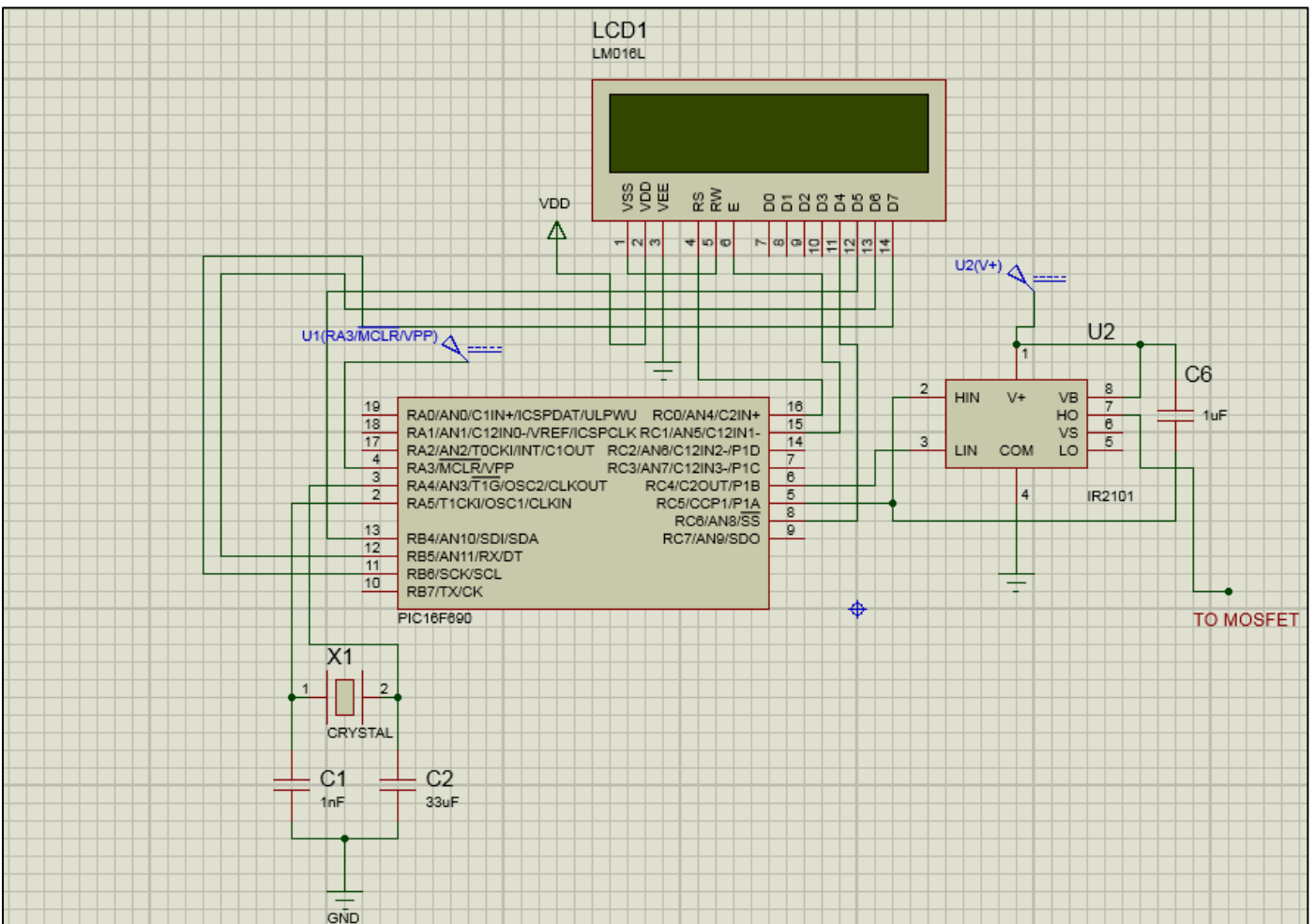


Fig 7 Interactive Simulator for Integrated Systems (ISIS) Circuit Implementation of the Control Circuit

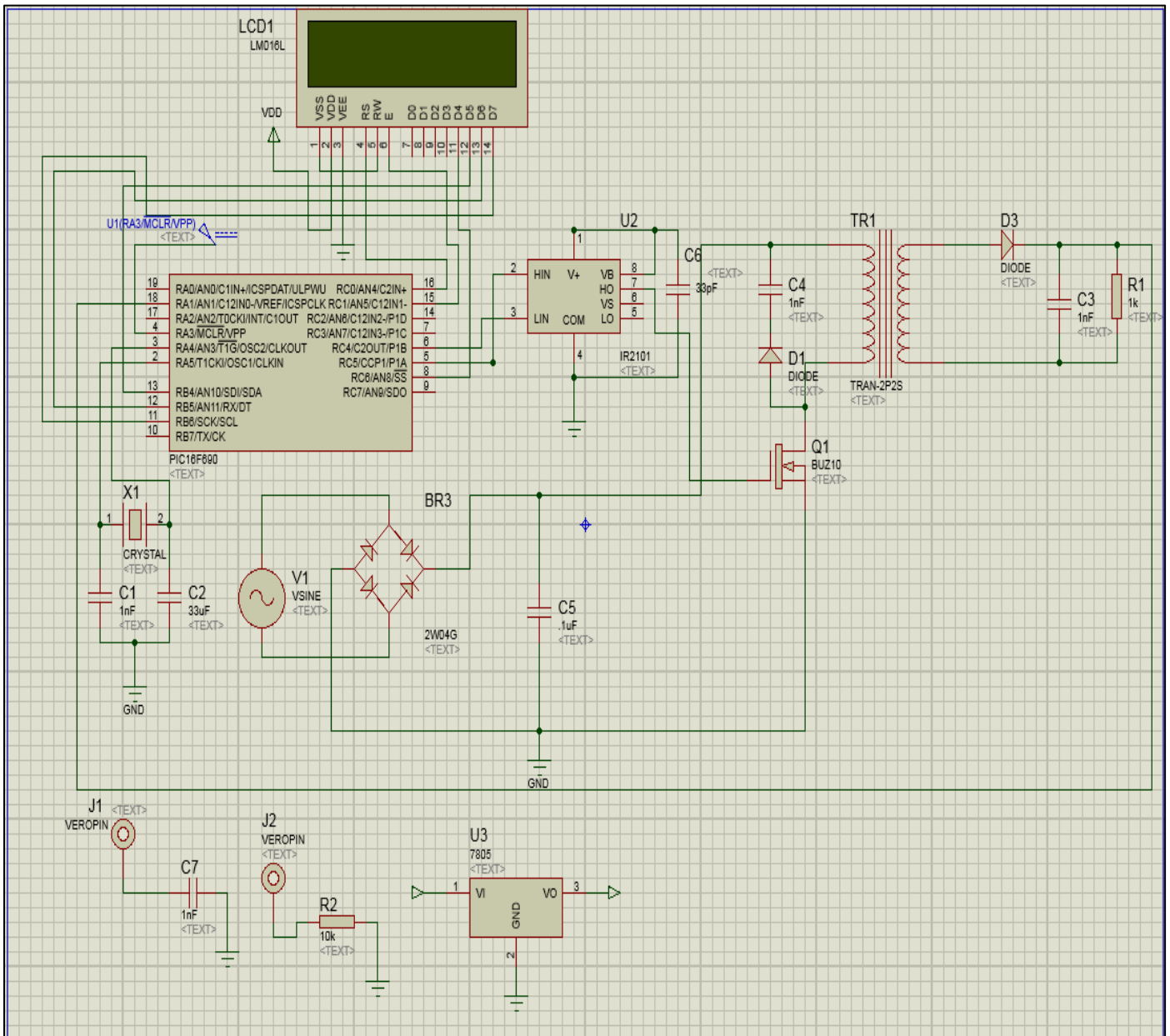


Fig 8 Interactive Simulator for Integrated Systems (ISIS) Fragment for Overall Bond

As seen by the preliminary circuit given in Figure 8 above, one can note that all the parts were currently accommodated in the ISIS drawing area. In addition, the values of the components were verified so that design mistakes would be reduced as much as possible. The diagram would be segmented for the layout of the drawing specifications, and the circuit design wanted to have. This aimed to avoid the wire capping and collisions in the system when interconnecting the components or sections.

Therefore, printed circuit boards were created and integrated to build the framework idea for a high-power, highly efficient DC converter. The overall goal was to design a high-power, high-efficiency DC power converter. This encompassed the complete process of converter design, including the schematic capture stage to map out the electronic circuitry and the printed circuit board (PCB) layout phase to determine the physical board on which the components and connections will be placed. The aim was to

integrate optimization of the power characteristics and efficiency with developing the converter's PCB from schematic to final board layout.

➤ *Diagrammatic Recording*

The Figure above shows that highly efficient high-power DC converter frameworks with various circuit pattern options were also laser engraved on the ISIS.

The entire assembly was later fabricated with the adoption of ISIS library files that had been added to the schematic to operationalize the DC converter design. ISIS library files provided all that is needed to turn the chosen design into the applied schematic.

➤ *PCB Layout*

This PCB layout has been developed with the help of ARES to make single or double-sided PCB layouts after schematic capture. The schematic capture is shown in Figure

5.10. Therefore, the schematic capture above is converted into a single or double-sided PCB layout using the ARES tool. However, we chose to AutoRoute the PCB layout into the double-sided PCB layout because the layout was two-sided. The PCB layout was AutoRoute. In particular, the single-sided PCB layout and prototype evidence of each segment (board) of the schematic capture must be completed to generate a well-drawn layout for a PCB. Such component rearrangement was necessary for their arrangement. All the parts of the segments or components that would produce the desired results must be adjacent to the PCB border, so it was easy and possible to access J1, J2, J3, J4, and J8 easily when they worked correctly. Consequently, segments of a PCB should be positioned close to its border; as a result of a good layout in terms of design, it was possible.

The PCB has been configured with automated routing from the schematic circuit design. Such rules during the design checking were modified according to the required designs that the DIL segments/ PCB components should have to enable efficient signal routing and achieve the preferred routing result. The ground planes around each leg of the element, as well as the leads, were removed on the PCB, and large through-hole squares were created to fit each

element, thereby increasing the degree of freedom in inserting and soldering with large DIL pads assigned for each significant element and sufficient and well-ordered soldering and simple drilling. The small components were first soldered so that the more critical components placed on the top side of the printed circuit board could subsequently be adequately soldered without issue. The blue tracks signified single-sided wires of conventional PCB layout ships, while the red tracks refer to the duplex designation of dual-sided wiring in the boat.

➤ *ARES Implementation*

After implementing the ISIS Proteus simulations, PCB manufacture follows the procedure after production. Unfortunately, another critical Proteus tool, ARES, must be used to create the schematic. This project must have a through-hole printed circuit board. Then, the schematic was created once parts were selected from the ARES library. Upon receipt by technicians, the file was used to produce the PCB board, which the team subsequently drilled, soldered the required components, and conducted. The required evaluations were conducted. The implementation diagram utilizing the ARES model is depicted in Figure 9 illustrates.

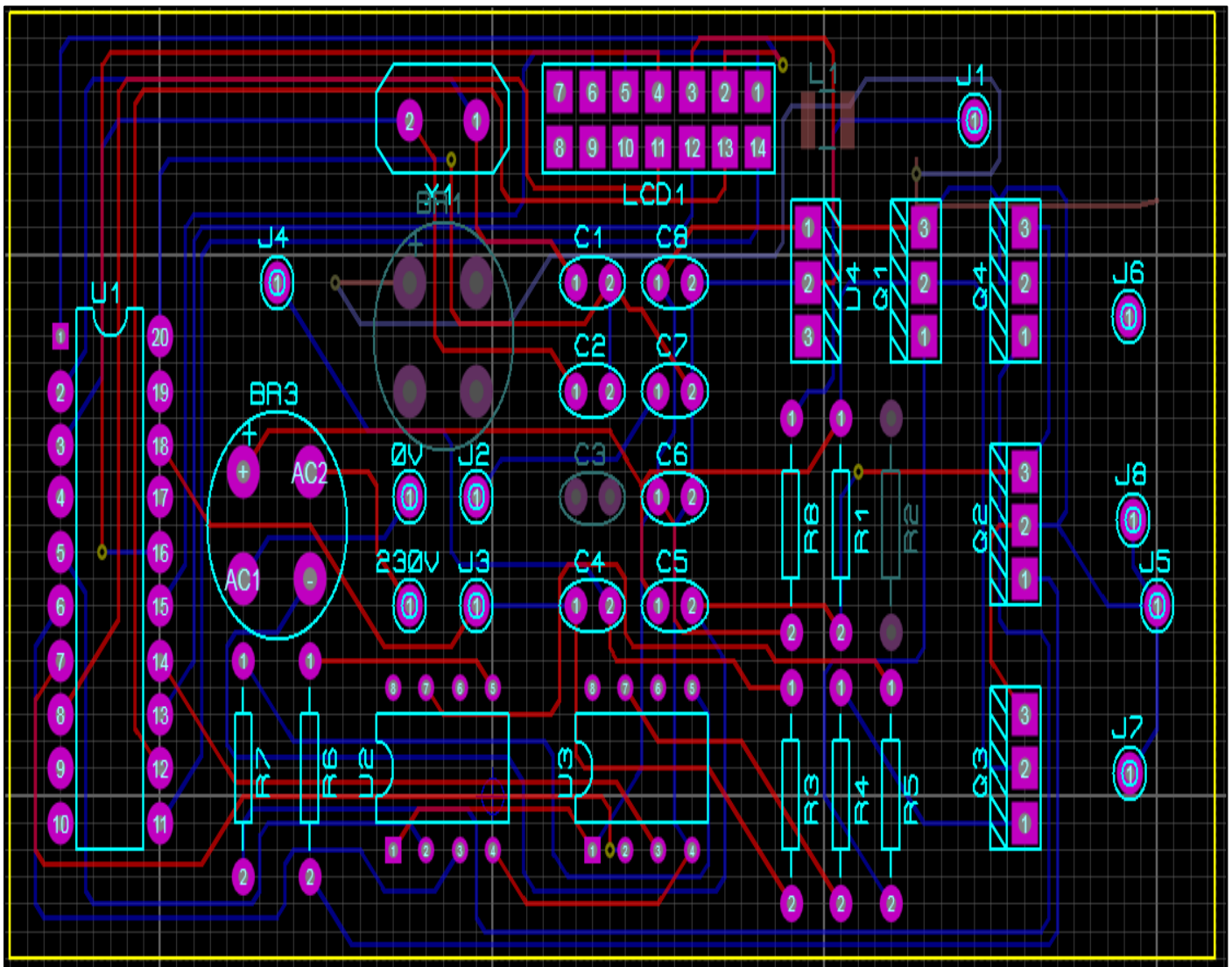


Fig 9 Complete Circuit Realization in ARES Mode

The ARES circuit and connecting of the components can be seen in Figure 9. on the other hand, the element PCB acts as the carrier medium for the conductor surface, which interfaces media between the element and interconnection circuitry. The J1, J2, and J8 wires interconnect the AC input and transformer on the PCB.

- Figure 10 shows the 3D Visualization Illustration of the ARES Design Indicated in Figure 9.

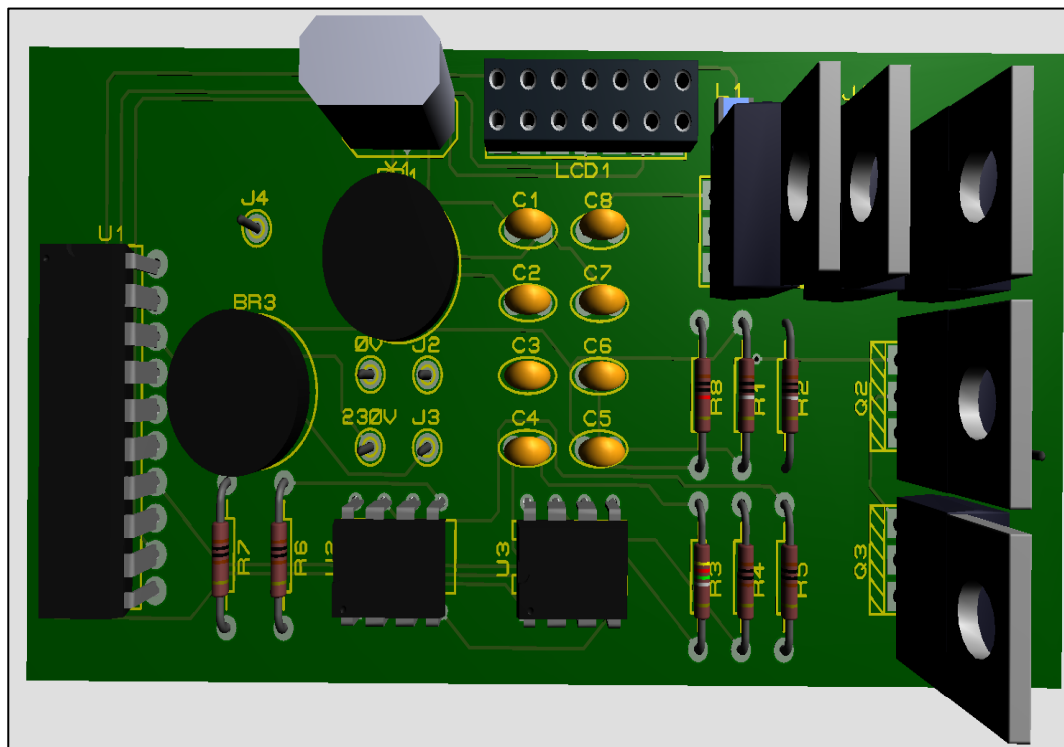


Fig 10 Circuit Picturing in 3D Using ARES

Figure 10 displays the circuit's 3D ARES representation with each component on the PCB board. The transformer was represented with the Vero pin and AC input side. All the elements of PCB implementation are shown in the 3D visualization. The printed circuit board (PCB) is fabricated with a double-sided layer.

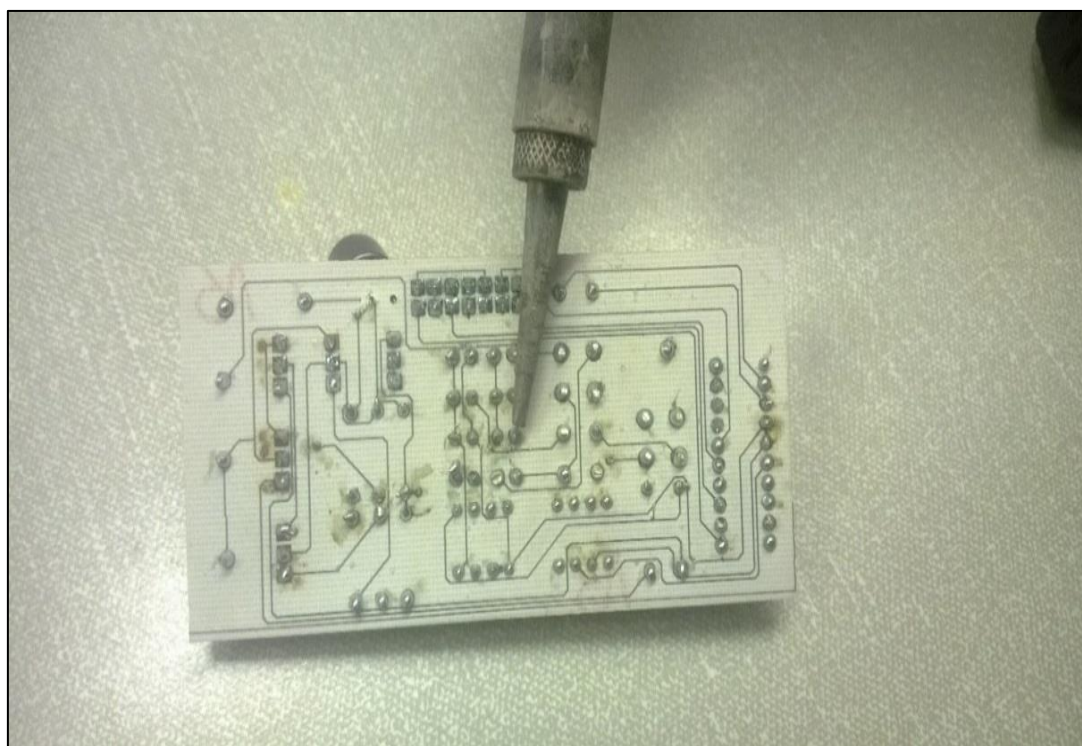


Fig 11 PCB being Soldered

Figure 11 shows the bottom view of the soldering of the components on the PCB. The components are soldered according to the design of the PCB.

➤ *MPLAB and ICD3 Implementation*

Correctly written codes of C programming under Hi-tech should be followed by download to the interface test board with MPLAB ICD3. The Figure below illustrates the download link to be connected.

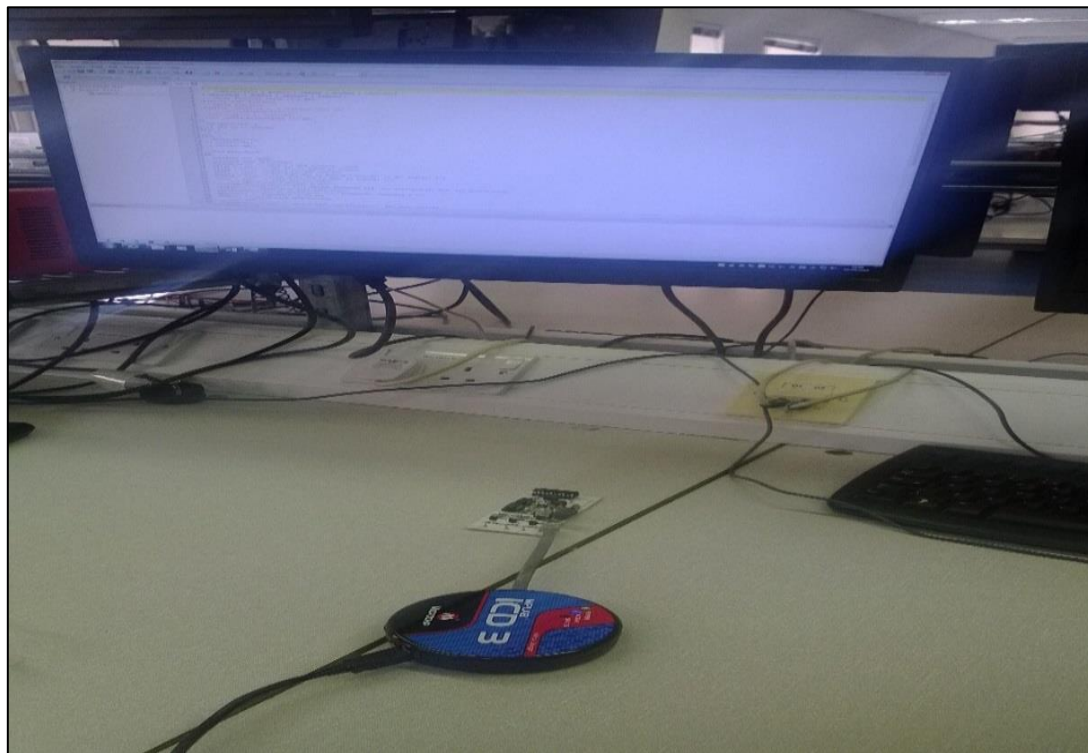


Fig 12 MPLAB Implementation with Interface Board

Given an inspection, the PCB components were soldered in the order of component sizes without inductors; after, the resistors and other smaller components followed other more significant elements such as inductors. Printed circuit board final image Circuit testing.

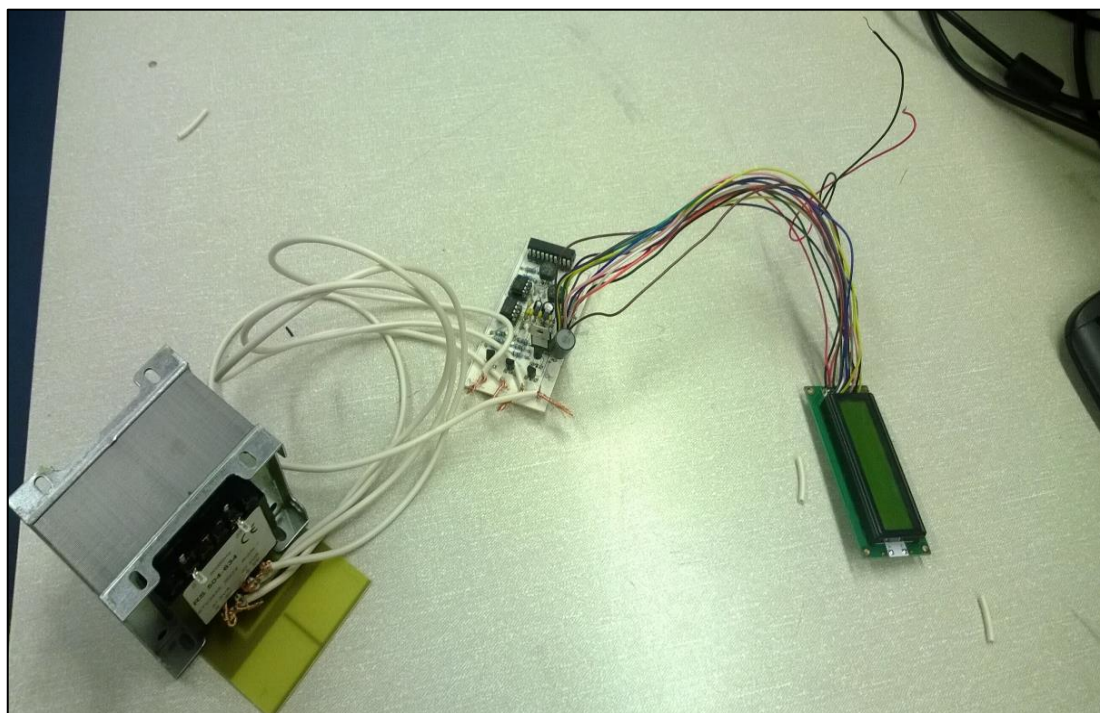


Fig 13 Printed Circuit Board Final Image

➤ *Circuit Testing*

Figure 12 is the graphical mode of circuit testing that follows an excellent soldering job and a bench test of the PCB circuit. The company's software validation process was instrumental in confirming the simulation findings. Figure 13 displays the power supply for the printed circuit board and the DC voltage electrical output that produced the results.

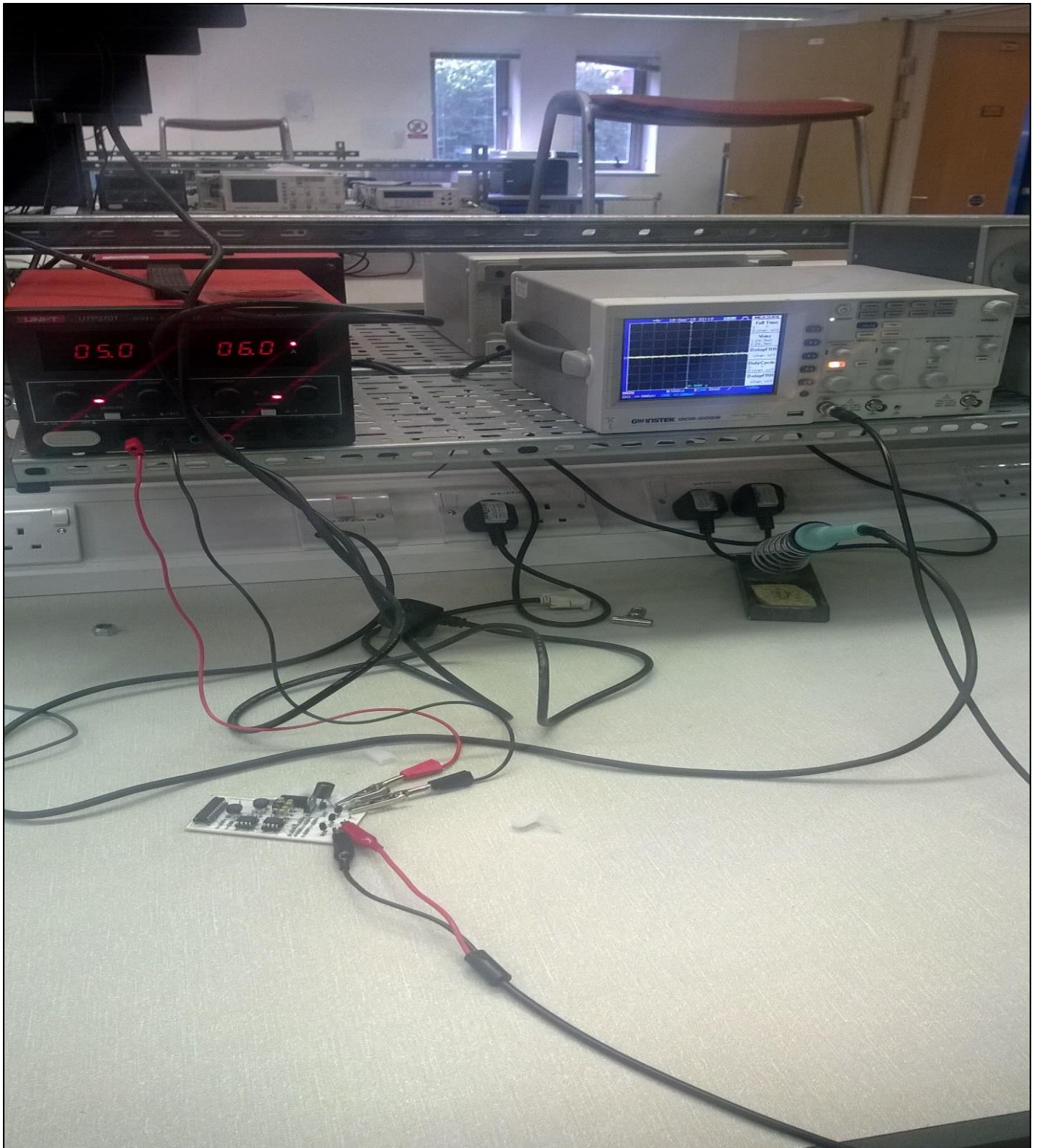


Fig 14 Indicates a Testing of the Circuit Diagram

➤ *Bill of Materials*

The components were delivered later to the technicians as requested within the allotted timeframes. This enabled the rapid soldering of the printed circuit board components and subsequent testing. The resources utilized in this scheme are itemized in Table 3.

Table 3 The List of Required Materials for Building a Dc Power Supply with One Phase

Description of each Component	Quantity	Price Per Unit (£)	Price Total in (£)
PIC16F690	one	1.56	1.56
Crystal (20 MHz)	one	1.48	1.48
Capacitor (1000uF)	One	0.126	1.134
Capacitor (1nF)	Three	0.114	0.342
Transformer	one	4.20	4.20
MOSFET	Five	0.212	1.06
Resistor (10Ω)	Four	0.026	0.104
Resistor (1kΩ)	Five	0.027	0.108
Capacitor (33pF)	Three	0.164	0.492
7805 regulators	One	0.476	0.476
IR2101	two	1.43	2.86
IN4007	Eight	0.027	0.216
Inductor(10mH)	One	1.506	1.506
LCD 16 by 2	one	4.57	4.57
Capacitor (10uF)	Nine	0.126	1.134
Summation			£21.088

Besides, the timelines for all stages and the estimated milestones of each stage vary.

In the forms and tables section of the appendix, a specially designed Gantt chart using Microsoft project is a short form drawn down fully.

IV. RESULTS

➤ Introduction

This discussion focusses on a detailed presentation of the results obtained in the course of the above practical and the analysis of these results to compare and contrast with the general aim of the study and the deliverables to determine the study’s success level as well as the limitations encountered.

➤ MATLAB Simulation Results

The AC input voltage waveform generated in MATLAB is input into the full bridge rectifier to produce the output voltage, as depicted in Figure 15. Rather than using MATLAB, an alternate option would be to utilize a function generator to supply the AC input signal to the rectifier circuit.

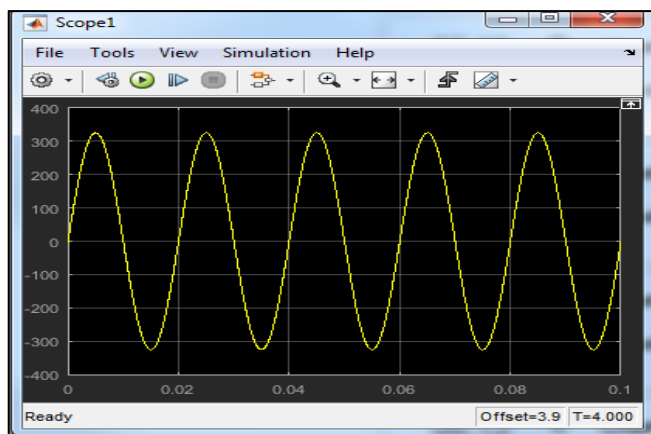


Fig 15 The output Waveform from a MATLAB Simulation Displaying the Behaviour of the Primary AC input Voltage Over Time

Fig. 15 shows the resultant value of an output voltage that can be seen from the simulated output impedance of 230-volt primary AC voltage rectifications to a full bridge rectifier. Second, the figures are represented by the waveform peaks-to-peaks ripple of 320 waveform dropouts. These values come from the mains voltage. The Matlab waveform is shown in Figure as the waveform of a full wave rectifier whose output voltage is 6. 2. It also represents the waveform obtained from the full wave rectifier for output voltage 16 and is shown as.

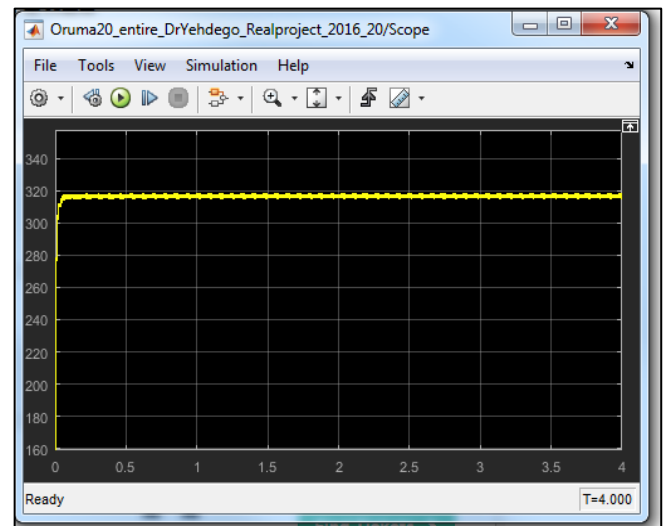


Fig 16 The Simulated output Waveform Generated in MATLAB to Model the Full Bridge Rectifier's Behaviour and Rectification Characteristics

Figure 16 displays the MATLAB simulation results of the full bridge rectifier, which produces the rectified output voltage from the rectifier circuit. The input used was 230V-rms (320V peak) from the mains, and the output from the rectifier was less than 320 V DC peak and smoother (Figure 15 and Figure 16). This voltage drop was due to the resistance created by the forward-biased diodes:

$$1.414 \times 230 = 325.22V$$

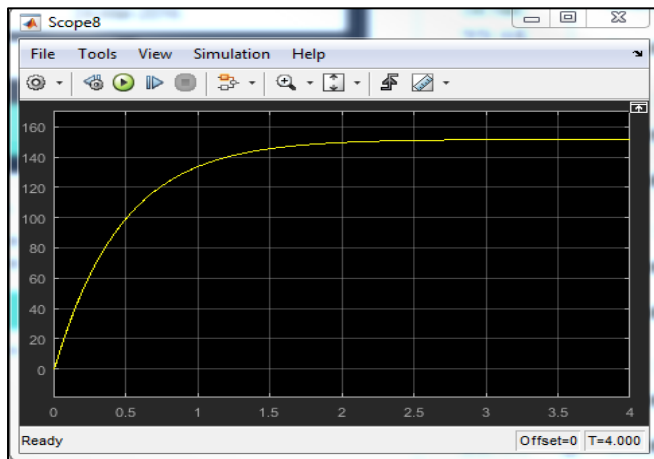


Fig 17 Simulation of Choke output Voltage Unit MATLAB

The Figure below offers insights into how the flyback converter, with its R-DS Vout, looks at the simplicity found after the transformer's secondary and after the secondary in the LCR filtering. The typical output of DC voltage, namely, 150V rating, appears to have a negligible difference with that, not resulting in zero or loss. Based on this claim, the power converter exhibits steady output voltage and current levels, along with the required regulation of the output voltage magnitude. This demonstrates the high-efficiency nature of the proposed converter over a converter in highly efficient DC source back flyback.

➤ *ISIS Simulation Results*

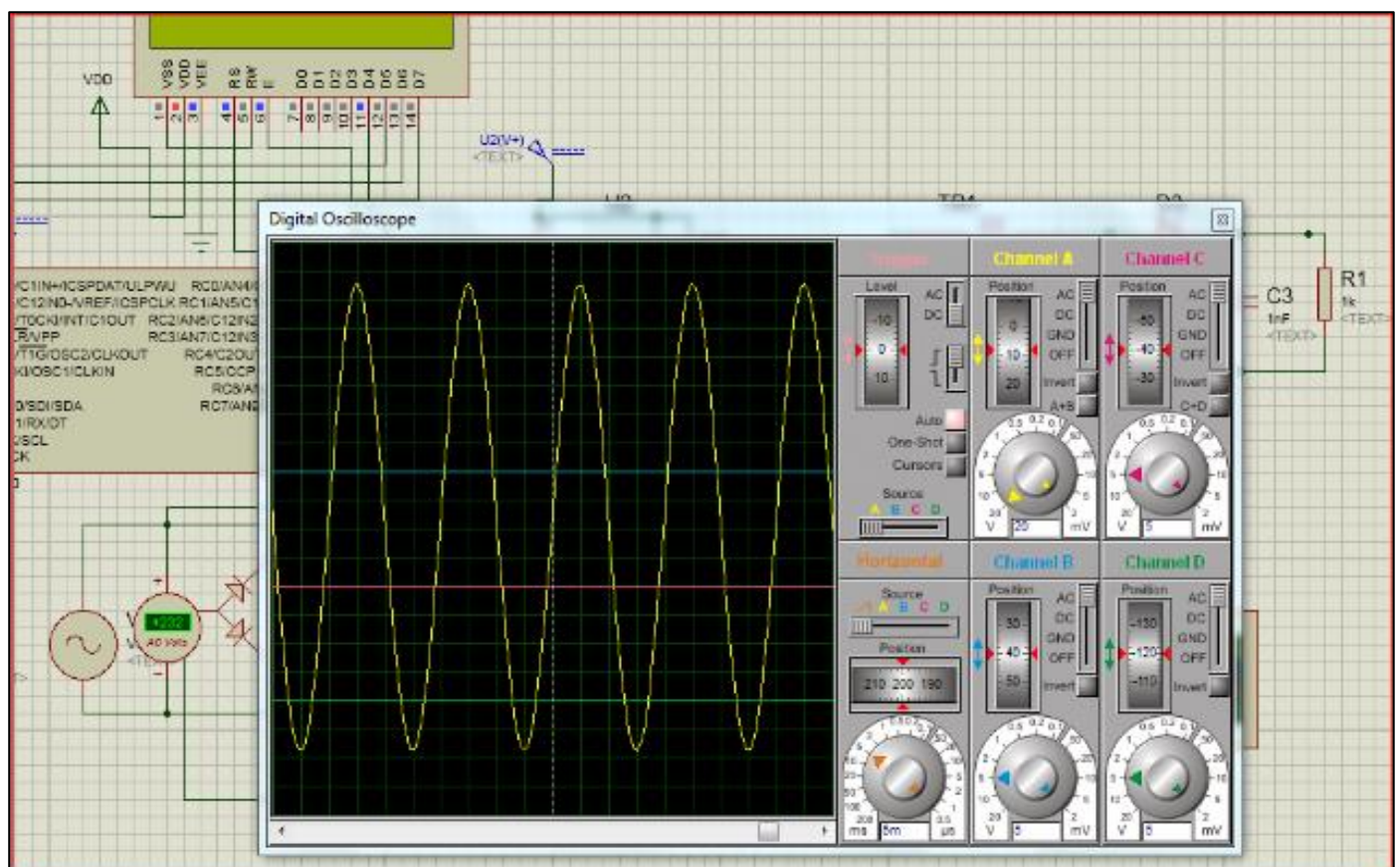


Fig 18 The Simulation Results of ISIS of main Grid Primary input Voltage

The simulation result of AC primary input voltage is based on the shape of Figure 18. The simulation record demonstration was conducted at a scale-down, i.e., 230 V rms to the input of the AC side. As a result, the input voltage waveform generated 320 p2p ripples from the mains, rectified at a rectifier's AC to the DC source, as illustrated below in Figure 19.

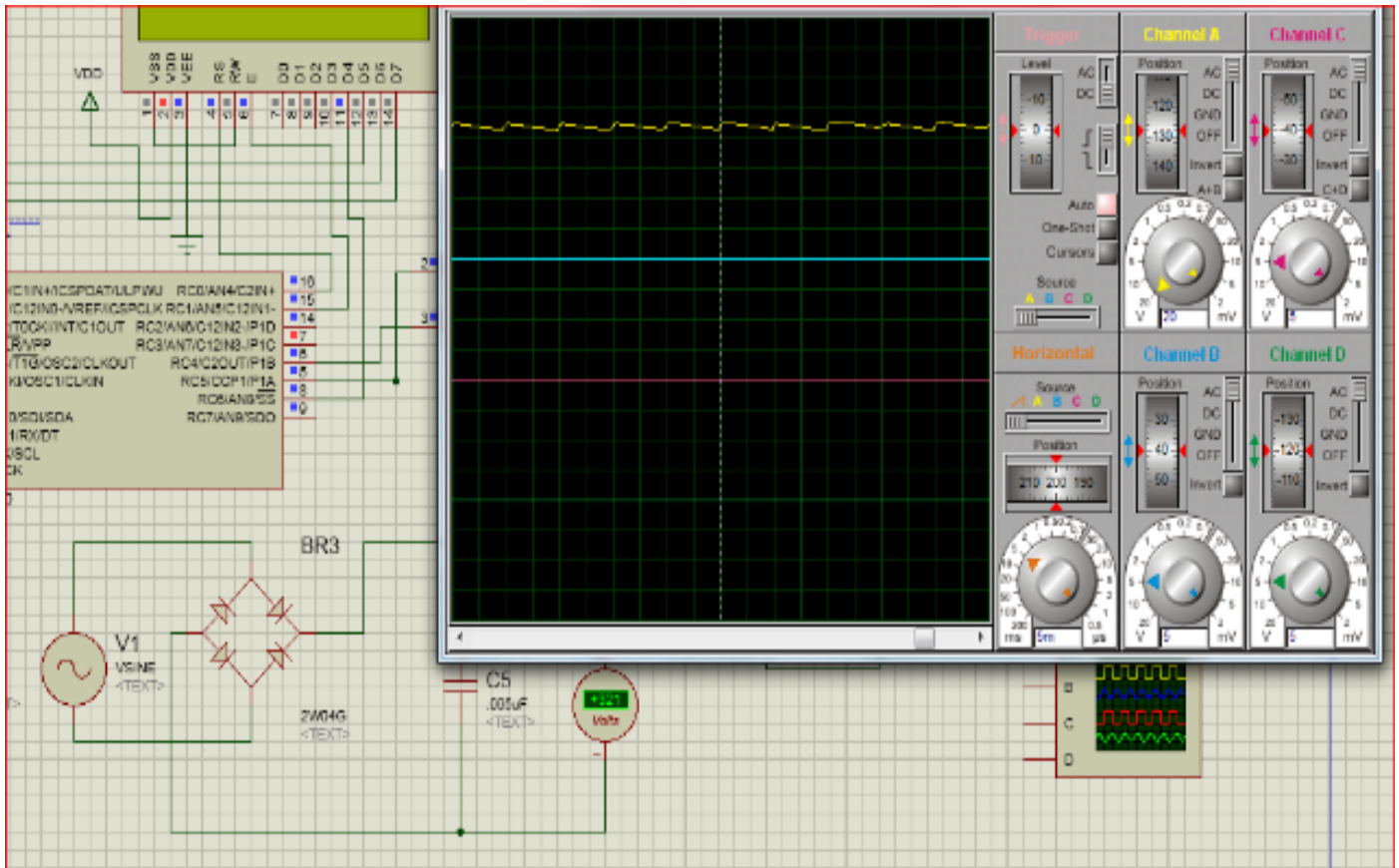


Fig 19 The Complete Bridge Rectifier's ISIS Simulation Result

- The choke's Simulation Result is Displayed in Figure 20.

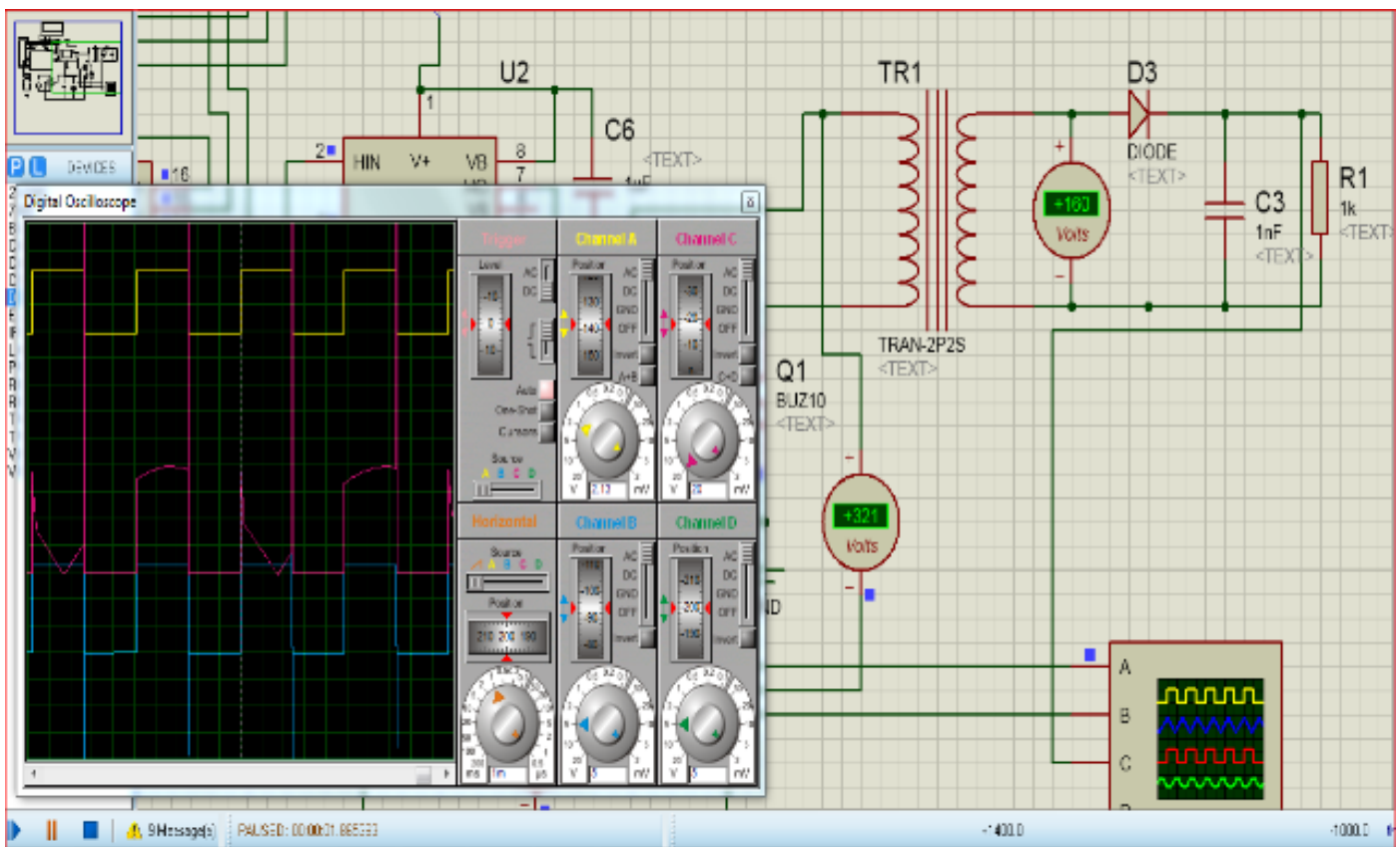


Fig 20 The Interactive Simulator for Integrated Systems (ISIS) output of the High-Frequency output Voltage (V)

The simulation outcome showed the rectifiers having an output of 321V, while the transformer voltage output was 160V. The transformer output voltage, represented by the pink waveform in Figure 20, displayed spikes and fluctuations. This unstable nature was attributed to utilizing a linear transformer rather than a mutual coupling transformer.

➤ *DSO Results*

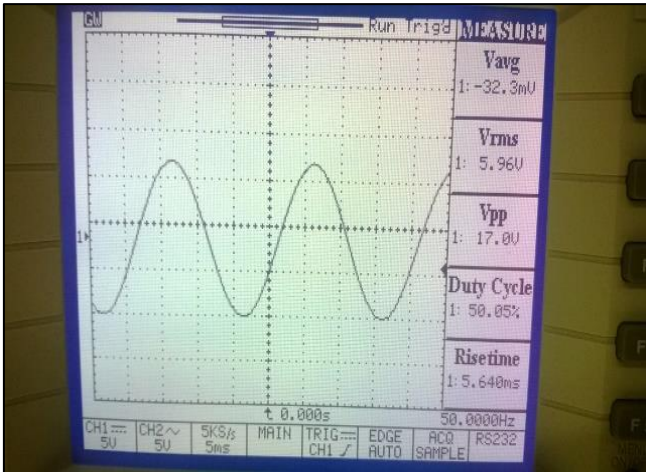


Fig 21 AC Primary input Voltage DSO Result

As shown in Figure 21, the DSO result represents 5.96 VAC scaled-down input voltage. The AC input voltage was then reduced from 230V rms to 5.96 V. Based on the DSO Volume, from the Top view, the DSO Result showed the peak voltage at $1.68 \times 5V$ on Channel 1 of the DSO. The result was 8.42V peak voltage, which is also approximately 5.96 when converted from peak voltage into rms (divided by 1.414). The rectifier output is shown in Figure 22.

The output also revealed a 50Hz frequency of the input signal and a 50.05% duty cycle. The input signal was a sinusoidal wave with no distortion to the input signal, and the distortion level was zero. This meant that it could be assumed to be accessible to ignore the harmonic distortion from the input voltage, and only the displacement factor should be considered.

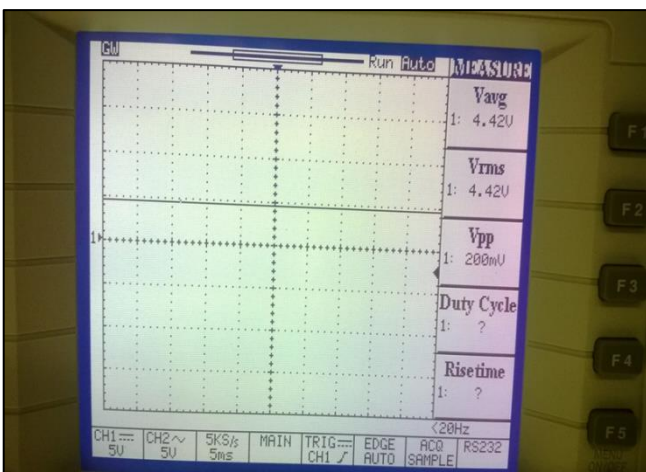


Fig 22 Digital Storage Oscilloscope (DSO) Results of Rectifier Output Voltage

- *The Depiction from the DSO (Digital Storage Oscilloscope)*
- *Figure 22: Digital Storage Oscilloscope (DSO) Results of Rectifier Output Voltage*

The depiction from the DSO (Digital Storage Oscilloscope) results for the scaled-down AC primary input voltage waveform, as exhibited in Figure 22, is the rectified voltage waveform for the output voltage reaching a peak of 5.96 V. Analyzing the measured voltage, averages the voltage of 4.42V can be observed. It appeared as a smooth waveform free from any ripple. However, there was a slight discrepancy between the measured and expected DC voltage of 5.36V as per the design calculations. This divergence can be attributed to the voltage drop observed in the IN4001 diode utilized in the circuit.

V. DISCUSSION

In this part, we will look at the results of the simulations and why it was impossible to perform the tests.

➤ *MATLAB Results*

- Initial input voltage of AC in primary (Figure 15) –
- Volts of rectifier output equivalents (Figure 16) –
- Primary Alternate Current (AC) input voltage – Figure 6.4
- The output voltage of the rectifier, as shown in Figure 15-
- DC output as a resultant after flyback —.

The rectifier displays a direct input-output voltage correlation in Figure 15, exhibiting only current voltage values. In comparison, Figure 16 presents the applied input and the resultant output voltage. The MATLAB assessment computed the rectifier efficiency at 95.3% for rounded waveforms, as depicted in Figure 6. The optimal operational point was attained based on the simulations conducted via MATLAB. The flyback converter efficiency measurements, as shown in Figure 6.3, also demonstrated a maximum of 100 %.

The value of ISIS was 99.07 per cent.. In Figure 15, the ISIS simulation is measured, and the efficiency of the output voltage rectifier is 98—77%. Figure 6.6 depicts the estimated flyback converter efficiency (ISIS simulation) at 106.7%.

➤ *Discussion of MATLAB Results*

The MATLAB simulation results compared different regimes for the primary AC input voltage (Figure 15)), rectifier the output voltage (Figure 16)), and the output flyback DC voltage (Figure 17)). It is also important to highlight that the differences between the measured values and the simulation results were mainly characterized by forward-blocking voltage featuring the diode that provoked calculation mistakes.

➤ Discussion of ISIS Results

Similarly, the Interactive Simulator for Integrated Systems (ISIS) simulation findings were separated into different stages for further analysis. Namely, these phases comprise - the principal input AC voltage feeding into the primary side, as exhibited in Figure 18; the rectified voltage signal output by the rectifier, as shown in Figure 15; and the direct current voltage delivered as output from the flyback converter secondary side, as portrayed in Figure 6.6. As a comparison between the efficiencies attained from MATLAB and ISICE, they were recorded at a lower rate than the results produced by MATLAB. Such a disparity, however, can be because the simulation results for ISIS strongly resemble real-life situations. However, it should be pointed out that the efficiency result of 106.7% observed from the ISIS simulation is unrealistic since it has been achieved through the modelling of mutual induction being used as a transformer for the flyback converter. In the case of real life, the efficiency would be reduced by a significant amount.

➤ Discussion of DSO Results

The rectified values given in the results of DSO were only used for the primary inbound AC input, as shown in Figures 6.7 and 6.8. However, the why argument will be presented in 5.4.5 on the impossibility of obtaining additional by DSO is presented in Section 5.4.5

➤ Discussion of Efficiency

Figure 15 shows MATLAB simulation showing the measured efficiency of the primary input AC recycler wh, where the efficiency is seen from the input voltage versus output voltage relationship in Fig.16. In addition, the efficiency measured for the output voltage rectifier, based on the MATLAB simulation, is 95.3%, as indicated in Figure 16 below. Lastly, the efficiency of the flyback converter obtained from Figure 17, which is calculated using MATLAB simulation, is 100%.

- *The Average MATLAB Efficiency is therefore Determined by:*

$$\text{Average MATLAB Efficiency} = (98.4\% + 95.3\% + 100\%) / 3 = 97.9\%$$

Similarly, ISIS found in the analysis that the computed efficiency was 99.07%, as shown in Figure 18. ISIS, meanwhile, offers the efficiency of the output voltage rectifier with 98.77% efficiency, as shown in Figure 15. Moreover, the flyback converter efficiency, the ISIS simulation given in Figure 6.6, calculated using the ISIS program, was found to be 106.7%.

- *The Mean Efficiency of ISIS = $0.9907 + 0.9877 + 1.067 / 3 = 1.0151$*

By and large, the efficiency of the MATLAB simulation was slightly less than the ISIS simulation by 3. % 7. The variance gap can be explained by the assumption of the linear transformer modelling the pulse transformer. However, from an engineering perspective, the data appear acceptable and consistent with the established expectations.

To conclude, the percentage of MATLAB utilized in the simulation was less than the value of the performance of the ISIS case by the difference of 101.51% minus 97.77%, which equals 3.74%. The discrepancy resulted from that linear transit until the pulse transformer. On the other hand, the effect appeared reasonable at the Engineering level. On the same note, acceptable results from the MATLAB simulations can be measured, albeit minor differences were noted between the ISIS simulations. It is good to stop testing the PCB and prevent it from proceeding beyond its primary AC input voltage rectifier. The following portion will determine the root reason behind the stated issue. Based on such root cause identification, we concentrate on rectifying this circuit and restoring it to regular functional cycles. The five inquiries demanding direct elucidation leverage the root cause analysis methodology to resolve the underlying problem. The analyses conducted were as follows:

- This is curious because it is evident that 4.42V is developed at the H-bridge converter input terminal. Still, no voltage will be generated across the output of the filter.
- What could be the reason the filter input has no voltage?
- Why don't MOSFETs' drain and source terminals have any voltage?
- Since voltage is present at the gate of one MOSFET of the 4-gate structure and at the lid of none of the other MOSFETs, what exactly determines the voltage at the gate of the sole MOSFET but not the rest of the MOSFETs?
- What is the reason why there is no output from the three pins of the Microcontroller unit?

References to microcontroller configurations are concerned; the PIC16F690 microcontroller was used, a user-friendly and flexible pin configuration microcontroller. Nonetheless, PWM outputs were hooked to pins P1A, P1B, P1c, and P1D. Port C programming of the microcontroller would see only one pin P1A support compared to capturing PWM (CCP). It is likely that beyond the P1A pin, further variations of the duty cycle would not be observed, for this would entail applying more advanced programming techniques to the remaining pins.

VI. CONCLUSION

As part of this study, a very efficient DC-to-DC converter was fabricated for DC drive motor applications. The goal of the leading research was to implement investigations, design, and construct a functional DC power supply that would suit the open-frame motors in the laboratory environment. Extensive investigations and discussions were conducted regarding the performance of the converter. Some study goals were successfully achieved, leading to a better understanding of PWM control. The simulation results obtained for the flyback converter were generally aligned with the expected theoretical outcomes, although slight differences were observed between the ISIS and MATLAB simulations.

Nonetheless, the simulation results indicated the need for constructing a test bed to validate the initially obtained results. Only DSO tests were employed for the construction of the test bed. Moreover, extensive results were obtained due to the circuit's improper functioning.

A few critical reasons were mentioned for the inability to validate the verified results. Mathematical computations of the efficiency of the ISIS and MATLAB simulations demonstrated the effective utilization of the flyback converter for stepping down DC voltage. In this research, the flyback converter operated in the step-down mode, employing a PWM duty cycle for DC voltage regulation through Proportional-Integral (PI) control.

FUTURE WORK

This research utilized an advanced DC-DC converter involving primary AC input voltage rectification, flyback conversion, and subsequent rectification, resulting in a complex configuration. On the other hand, the looking-ahead tradeoffs include minor tradeoffs for more straightforward options and a less precise DC feed. This would involve using a lightweight single DC chopper circuit, the PWM duty cycle of which varies. Besides using the flyback converter to convert voltage from high to low, it can also be used to reverse the process and restore from a low voltage to a high voltage and remain relatively cheap. The buck-only mode was used during the processing of this work. Improving the C code's step-up functionality, which allows for PWM variation through feedback loop control, will be required in future undertakings.

REFERENCES

- [1]. Gopi, e. a. (2014). High step-up isolated efficient single switch DC-DC converter for a renewable energy source. *Ain Shams Engineering*, 5(4), 1115–1127.
- [2]. Gopi, R. Saravanakumar. (2014). High step-up isolated efficient single switch DC-DC converter for a renewable energy source. *Ain Shams Engineering*, 5(4), 1115–1127.
- [3]. Amin Mirzaei al. (2011). Design and implementation of high-efficiency, non-isolated bi-directional zero voltage transition pulse width modulated DC–DC converters. *Asia-Pacific Forum on Renewable Energy*, 47(1), 358–369.
- [4]. at., R.-J. e. (2012). High-Efficiency DC–DC Converter With Two Inputs. *IEEE TRANSACTIONS ON POWER ELECTRONICS*, 27(4), 1862-1869.
- [5]. Attar Zadeh. (2008). A new direction in project management success: Base on brilliant methodology selection. *Information Technology*, 2008. ITSIm 2008. International Symposium. 1, pp. 1 - 9. Kuala Lumpur: IEEE.
- [6]. Ben Guo et al. (2013). Control of three-phase buck-type rectifier in discontinuous current mode. (pp. 4864 - 4871). IEEE.
- [7]. Bin et al. (2013, April). High Boost Ratio Hybrid Transformer DC-DC Converter For Photovoltaic Module Applications. *IEEE TRANSACTIONS ON POWER ELECTRONICS*, 28(4).
- [8]. Bindra, A. (2014). <http://www.digikey.co.uk/en/articles/techzone/2014/jan/high-voltage-dc-distribution-improves-data-centre-system-efficiency>. Retrieved November 30, 2014, from <http://www.digikey.co.uk/en/articles/techzone/2014/jan/high-voltage-dc-distribution-improves-data-centre-system-efficiency>
- [9]. Blundell et al. (2002, June 06). AC-DC converter with unity power factor and minimum harmonic content of line current: design considerations. *Electric Power Applications, IEE Proceedings*, 145(6), 553 - 558.
- [10]. Cho, Y.-W. (2014, April 30). Single Power-Conversion AC--DC Converter With High Power Factor and High Efficiency. *Power Electronics, IEEE Transactions*, 29(9), 4797 - 4806.
- [11]. Continetti, D. J. (2013). *Analysis and Design of High Efficiency, High Conversion Ratio, DC-DC Power Converters* (1st ed.). Colorado: University of Colorado.
- [12]. Daniel O et al. (2013). Efficiency analysis of a sliding-mode controlled quadratic boost converter. *ET Power Electron*, 6(2), 364-373.
- [13]. Dawson et al. (2002, August 06). DC-DC converter interphase transformer design considerations: volt-seconds balancing. *Magnetics, IEEE Transactions on*, 26(5), 2250 - 2252.
- [14]. Engel et al. (2004, August 26). Comparison of the Modular Multilevel DC Converter and the Dual-Active Bridge Converter for Power Conversion in HVDC and MVDC Grids. *Power Electronics, IEEE Transactions*, 30(1), 124 - 137.
- [15]. Horiuchi et al. (2008, June 24). Operation of the high-frequency half-wave rectifier circuit, which contains a saturable core. *Magnetics in Japan, IEEE Translation Journal*, 2(6), 512 - 513.
- [16]. Hsuan-Ju Chen et al. (2015). 20.9 An energy-recycling three-switch single-inductor dual-input buck/boost DC-DC converter with 93% peak conversion efficiency and 0.5mm² active area for light energy harvesting. *Solid- State Circuits Conference - (ISSCC)* (pp. 1 - 3). San Francisco, CA : IEEE.
- [17]. Hu et al. (2012, MAY 31). A Modified High-Efficiency LLC Converter With Two Transformers for Wide Input-Voltage Range Applications. *IEEE Power Electronics Society*, 28(4), 1946 - 1960.
- [18]. Itoh et al. (2002, August 07). Single-switch single-phase rectifier for step-down AC-DC conversion. *Electronics Letters*, 37(5), 276 - 278.
- [19]. Jiang et al. (2010, July 08). AC-DC-DC isolated converter with bidirectional power flow capability. *Power Electronics, IET*, 3(4), 472 - 479.
- [20]. Karl H. Edelmoser. (2005). High Efficiency DC-to-AC Power Inverter with Special DC. *AUTOMATIKA*, 3(4), 143–148.

- [21]. Kun-Huai et al. (2013). High-Efficiency Single-Input Multiple-Output DC-DC Converter. *IEEE TRANSACTIONS ON POWER ELECTRONICS*, 28(2), 886 - 898.
- [22]. Kun-Huai Jheng et al. (2012, February 20). High-Efficiency DC-DC Converter With Two Input Power Sources. *Power Electronics, IEEE Transactions*, 27(4), 1862 - 1875.
- [23]. Li W et al. (2007, May 29). ZVT interleaved boost converters for high-efficiency, high step-up DC-DC conversion. *Electric Power Applications, IET*, 1(2), 284 - 290.
- [24]. Lin, C.-Y. W.-J. (2005). High-efficiency, high-step-up DC-DC convertor for fuel-cell generation system. *Electric Power Applications, IEE Proceedings*, 152(5), 1371 - 1378.
- [25]. Machado et al. (2006, November 13). A Line-Interactive Single-Phase to Three-Phase Converter System. *IEEE TRANSACTIONS ON POWER ELECTRONICS*, 21(6), 1628 - 1636.
- [26]. Metwally et al. (2010, July 12). D-Dot Probe for Fast-Front High-Voltage Measurement. *Instrumentation and Measurement, IEEE Transactions*, 59(8), 2211 - 2219.
- [27]. Nathabhat Phankong, N. Y. (2014). Design of Power Rectifier Circuit for Three-Level Back-to-Back Converter. 56, pp. 574 – 583. *Energy Procedia*.
- [28]. Nicolae-Daniel et al. (2012). Control a 6/4 switched reluctance motor by a DC voltage supply with a DC high voltage intermediary circuit. *Electrical and Power Engineering (EPE), 2012 International Conference and Exposition* (pp. 419 - 426). Iasi: IEEE.
- [29]. Pruitt, D.L, et al. (2005, August 09). High-voltage DC power conditioner. *Electron Devices, IEEE Transaction*, 26(10), 1391 - 1393.
- [30]. Rafferty et al. (2015, March 19). Analysis of voltage source converter-based high-voltage direct current under DC line-to-earth fault. *Power Electronics, IET*, 8(3), 428 - 438.
- [31]. Reusch D et at. (2013). Understanding the effect of PCB layout on circuit performance in a high-frequency gallium nitride-based point of load converter. *Applied Power Electronics Conference and Exposition (APEC)* (pp. 649 - 655). Long Beach, CA: IEEE.
- [32]. Rong- Jong et al. (2012). High-Efficiency DC-DC Converter With Two Input. *IEEE TRANSACTIONS ON POWER ELECTRONICS*, 27(4), 1862-1869.
- [33]. Rong-Jong ,et al. (2008). High-Efficiency Power Conversion System for Kilowatt-Level Stand-Alone Generation Unit With Low Input Voltage. *Industrial Electronics, IEEE Transactions*, 55(10), 3702 - 3714.
- [34]. Rong-Jong et al. (2012). High-Efficiency DC-DC Converter With Two Input. *IEEE TRANSACTIONS ON POWER ELECTRONICS*, 27(4), 1862-1869.
- [35]. Ryoo et al. (2013, August 02). Design of high voltage capacitor charger with improved efficiency, power density, and reliability. *IEEE Dielectrics and Electrical*, 20(4), 076 - 1084.
- [36]. Shridhar. (2014). Design and simulation of an efficient traffic light controller (PTLC). *Computing for Sustainable Global Development (INDIACom)* (pp. 348 - 352). New Delhi: IEEE.
- [37]. Shuobo Xu et al. (2011). Project Management Methodologies: Are they sufficient to develop quality software? *Emergency Management and Management Sciences (ICEMMS)* (pp. 175 - 178). Beijing: IEEE.
- [38]. Stratakos, A. J. (2014). High-Efficiency Low-Voltage DC-DC Conversion for Portable. California: University of California, Berkeley. Retrieved from <http://citeseerx.ist.psu.edu/viewdoc/download;jsessionid=D7EC3286966606B323310D9176093A55?doi=10.1.1.91.8234&rep=rep1&type=pdf>
- [39]. Suk-Ho Ahn et al. (2014, October 21). Low-Ripple and High-Precision High-Voltage DC Power Supply for Pulsed Power Applications. *Plasma Science, IEEE Transactions*, 42(10), 3023 - 3033.
- [40]. Suma Umesh et al. (2014). Active power factor correction technique for single phase full bridge rectifier. *Advances in Energy Conversion Technologies (ICAECT)* (pp. 130 - 135). IEEE.
- [41]. Swetha. (2013). Design of DC link filter and inverter output filter for induction motor drive system. *International of Engineering science invention*, 2(1), 06-12. Retrieved from www.ijesi.org
- [42]. Tsornng-Juu Liang et al. (2014, December 25). Novel High-Conversion-Ratio High-Efficiency Isolated Bidirectional DC-DC Converter. *Industrial Electronics, IEEE Transactions*, 62(7), 4492 - 4503.
- [43]. Wai et al. (2005, September 09). High-efficiency, high-step-up DC-DC converter For fuel-cell generation systems. *Electric Power Applications, IEE Proceedings*, 152(5), 1371 - 1378.
- [44]. Wai, R.-J, et al. (2005, September 09). High-efficiency, high-step-up DC-DC Converter for fuel-cell generation system. *Electric Power Applications, IEE Proceedings*, 152(5), 1371 - 1378.
- [45]. Wai, R.-J. (2014). High-efficiency dual-input Interleaved DC-DC Converter for Reversible Power Sources. *Power Electronics, IEEE Transactions*, 29(6), 2903 - 2921.
- [46]. Xinke Wu et al. (2006, September 06). Analysis and Optimal Design Considerations for an Improved Full Bridge ZVS DC-DC Converter With High Efficiency. *Power Electronics, IEEE Transactions*, 21(5), 1225 - 1234.
- [47]. Yuan-Liang Li et al. (2013). Fast signal integrity methodology for PCB pre-layout analysis and layout quality check. *Electronic Components and Technology Conference* (pp. 2012 - 2017). Las Vegas: IEEE.
- [48]. Zhan Wang et al. (2013, March 15). An Integrated Three-Port Bidirectional DC-DC Converter for PV Application on a DC Distribution System. *Power Electronics, IEEE Transactions*, 28(10), 4612 - 4624.
- [49]. Zhao, J. J. (2010, July). AC-DC-DC isolated converter with bidirectional power flow capability. *Power Electronics, IET*, 3(4), 472 - 479.

- [50]. Daniel, W.H., (1997). "Introduction to Power Electronics." Prentice Hall International, Inc.: Valparaiso University, Indiana. 1 – 232.
- [51]. S. Zainal and J. Awang. (2009) "Power Electronics and Drives ."Faculty of Electrical Engineering, UTM Skudai: Johor. 27 – 30.
- [52]. O.P Arora. (2007) "Power Electronics Laboratory. Theory, Practise and Organization." Alpha Science: India. 71 – 79.
- [53]. Bernardo, P. C. (2009). A high-efficiency micro-controlled buck converter with maximum PowerPoint tracking for photovoltaic systems. Proceedings of the
- [54]. International Conference on Renewable Energies and Power Quality.
- [55]. Mrabti, T. (2009). Regulation of Electric Power of Photovoltaic Generators with DC-DC Converter (Buck Type) and MPPT Command. ICMCS '09. International Conference on Multimedia Computing and Systems, 322-326.
- [56]. Shanthi, T. (2007). Power Electronic Interface for Grid-Connected PV array using Boost Converter and Line-Commutated Inverter with MPPT. Proceedings of the IEEE International Conference on Intelligent and Advanced Systems, 882-886.
- [57]. Morales-Saldana, J. A. (2006). Modeling and Control of a Cascaded Boost
- [58]. Converter with a Single Switch. IECON 2006 - 32nd Annual Conference on IEEE Industrial Electronics, 591-596.
- [59]. Nabulsi, A. A. (2009). A 300 Watt Cascaded Boost Converter Design for Solar Energy Systems. EPECS '09. International Conference on Electric Power and Energy Conversion Systems, 1-4.
- [60]. S. Bang, D. Swank, A. Rao, W. McIntyre, Q. Khan, and P. K. Hanumolu, "A 1.2A 2MHz tri-mode Buck-Boost LED driver with feedforward duty cycle correction," in *Custom Integrated Circuits Conference (CICC), 2010 IEEE*, 2010, pp. 1-4.
- [61]. H. Yuequan, L. Huber, and M. M. Jovanovic, "Single-Stage Flyback Power-Factor- Correction Front-End for HB LED Application," in *Industry Applications Society Annual Meeting, 2009. IAS 2009. IEEE*, 2009, pp. 1-8.
- [62]. Min and S. Jian, "Feedforward current control of boost single-phase PFC converters," *Power Electronics, IEEE Transactions on*, vol. 21, pp. 338-345, 2006.
- [63]. G. Lamar, A. Fernandez, M. Arias, M. Rodriguez, J. Sebastian, and M. M. Hernando, "Limitations of the Flyback Power Factor Corrector as a One-Stage Power Supply," in *Power Electronics Specialists Conference, 2007. PESC 2007. IEEE*, 2007, pp. 1343-1348.
- [64]. P. T. Prathapan, C. Min, and S. Jian, "Feedforward current control of boost-derived single-phase PFC converters," in *Applied Power Electronics Conference and Exposition, 2005. APEC 2005. Twentieth Annual IEEE*, 2005, pp. 1716-1722 Vol. 3.
- [65]. Zhou and M. Jovanovic, "Design Tradeoffs in Continuous Current-mod.